



# Chapter 1

A short introduction to microphysics in the NWP ICON model

AXEL SEIFERT  
Deutscher Wetterdienst, Offenbach  
email: axel.seifert@dwd.de

February 2010

A short summary of the cloud physics is given for the non-hydrostatic branch of the ICON atmosphere model ICONAM. This parameterization is taken from the COSMO model, therefore the reader might also be referred to Doms and Schättler (2004).

## 1. Grid-scale clouds

ICONAM uses a two-category ice scheme which explicitly predicts the mass fractions of cloud water  $q_c$ , rain water  $q_r$ , cloud ice  $q_i$  and snow  $q_s$  at every grid point and includes the advection of all hydrometeors. For the non-precipitating categories we apply the budget equation including turbulent fluxes  $\mathbf{F}^{c,i}$ , but neglecting sedimentation:

non-precipitating categories (cloud water and cloud ice)

$$\frac{\partial q^{c,i}}{\partial t} + \mathbf{v} \cdot \nabla q^{c,i} = S^{c,i} - \frac{1}{\rho} \nabla \cdot \mathbf{F}^{c,i}, \quad (1.1)$$

While for precipitation-sized particles only sedimentation is taken into account, since for larger particles the sedimentation fluxes are usually much larger than the turbulent fluxes:

precipitating categories (rain, snow and graupel)

$$\frac{\partial q^{s,r}}{\partial t} + \mathbf{v} \cdot \nabla q^{s,r} - \frac{1}{\rho} \frac{\partial \rho q^{s,r} v_T^{s,r}}{\partial z} = S^{s,r}, \quad (1.2)$$

Figure 1.1 gives an overview of the microphysical sources and sinks  $S$  that are considered in this two-category ice scheme. The individual microphysical processes are:

$S_c$       condensation and evaporation of cloud water

$S_{au}^c$	autoconversion of cloud water to form rain
$S_{ac}$	accretion of cloud water by raindrops
$S_{ev}$	evaporation of rain water
$S_{nuc}$	heterogeneous nucleation of cloud ice
$S_{frz}^c$	nucleation of cloud ice due to homogeneous freezing of cloud water
$S_{dep}^i$	deposition growth and sublimation of cloud ice
$S_{melt}^i$	melting of cloud ice to form cloud water
$S_{au}^i$	autoconversion of cloud ice to form snow due to aggregation
$S_{aud}$	autoconversion of cloud ice to form snow due to deposition
$S_{agg}$	collection of cloud ice by snow (aggregation)
$S_{rim}$	collection of cloud water by snow (riming)
$S_{shed}$	collection of cloud water by wet snow to form rain (shedding)
$S_{cri}^i$	collection of cloud ice by rain to form snow
$S_{cri}^r$	freezing of rain due to collection of cloud ice to form snow
$S_{frz}^r$	freezing of rain due heterogeneous nucleation to form snow
$S_{dep}^s$	deposition growth and sublimation of snow
$S_{melt}^s$	melting of snow to form rain water

The following main assumption are made in the parameterization:

- The raindrops are assumed to be exponentially distributed with respect to drop diameter  $D$ :

$$f_r(D) = N_0^r \exp(-\lambda_r D), \quad (1.3)$$

where  $N_0^r = 8 \times 10^6 \text{ m}^{-4}$  is an empirically determined distribution parameter (Marshall-Palmer distribution). For the terminal fall velocities of raindrops as functions of size we use the following empirical relation

$$v_T^{rp}(D) = v_0^r D^{1/2} \quad (1.4)$$

where  $v_0^r = 130 \text{ m}^{1/2} \text{ s}^{-1}$ .

- The autoconversion scheme is parameterized using Seifert and Beheng (2001) which reads

$$\left. \frac{\partial L_r}{\partial t} \right|_{au} = \frac{k_{cc}}{20 x^*} \frac{(\nu + 2)(\nu + 4)}{(\nu + 1)^2} L_c^4 N_c^{-2} \left[ 1 + \frac{\Phi_{au}(\tau)}{(1 - \tau)^2} \right] \quad (1.5)$$

with  $L_{c/r}$  cloud/rain water content,  $N_c$  cloud droplet number concentration,  $\nu$  shape parameter,  $k_{cc} = 9.44 \times 10^9 \text{ s}^{-1} \text{ kg}^{-2} \text{ m}^3$ ,  $x^* = 2.6 \times 10^{-10} \text{ kg m}^{-3}$ . The function  $\Phi_{au}(\tau)$  describes the aging (broadening) of the cloud droplet distribution as a function of the dimensionless internal time scale

$$\tau = 1 - \frac{L_c}{L_c + L_r}$$

(for details see Seifert and Beheng 2001). In the one-moment schemes of the ICON model we simplify the scheme by assuming a constant cloud droplet number concentration of  $N_c = 5 \times 10^8 \text{ m}^{-3}$  and a constant shape parameter  $\nu = 2$ .

- Snow particles are interpreted as unrimed or partly rimed aggregates. The equation

$$m = \alpha D_s^2 \quad (1.6)$$

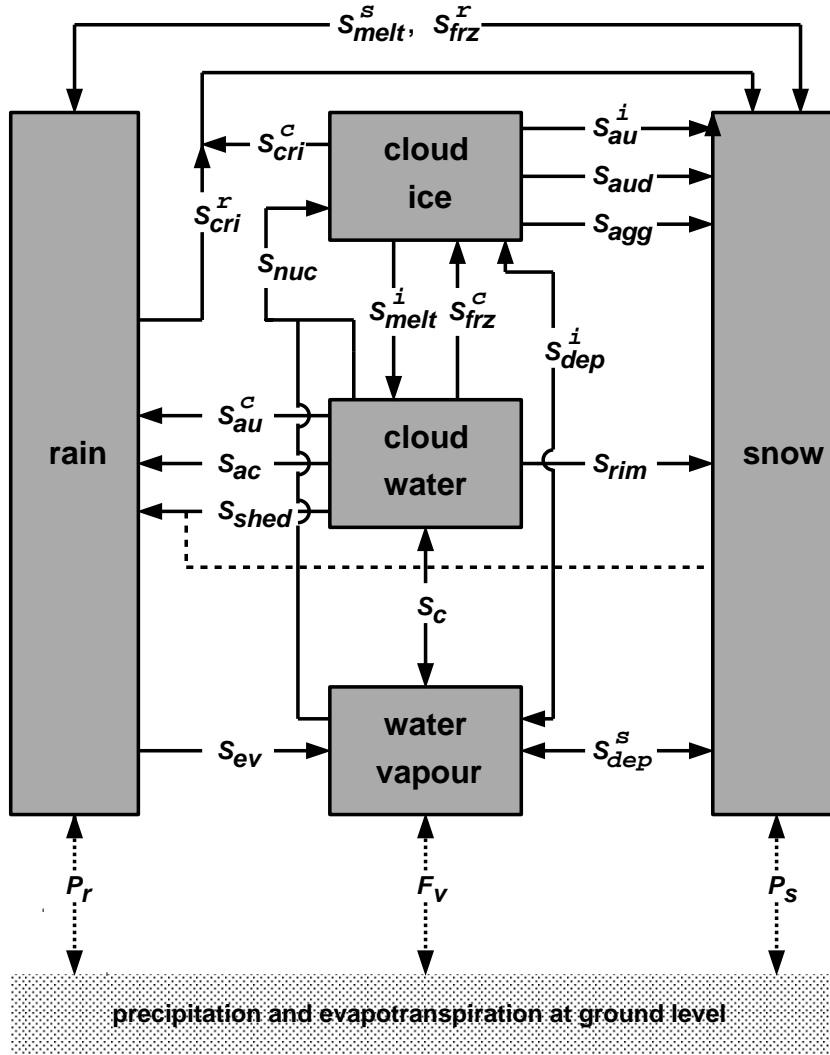


Figure 1.1: Cloud microphysical processes considered in the two-category ice scheme

with  $\alpha = 0.069$  is used to specify their mass-size relation and the terminal fall velocity is parameterized as  $v = 15 D^{1/2}$  (here  $D$  in m,  $m$  in kg and  $v$  in m/s). The size distribution of snow is an inverse exponential

$$f(D) = N_{0,s} \exp(-\lambda D).$$

The intercept parameter is parameterized as a function of temperature  $T$  and snow mixing ratio  $q_s$  by:

$$N_{0,s} = \frac{27}{2} a(3, T) \left( \frac{q_s}{\alpha} \right)^{4-3b(3, T)}$$

The functions  $a(3, T)$  and  $b(3, T)$  are given by Table 2 of Field et al. (2005). This parameterization is used instead of the constant  $N_{0,s} = 8 \times 10^5 \text{ m}^{-4}$  which was used in the old version of the scheme. Especially at cold temperatures the new formulation leads to a much higher intercept parameter, this corresponds to smaller snowflakes at high levels which fall out much slower. The choices about the size distribution and fall speeds of snow are very important for wintertime orographic precipitation.

- The rate of autoconversion from cloud ice to snow due to cloud ice crystal aggregation ( $S_{au}^i$ )

is parameterized by the simple relations

$$S_{au}^i = \max\{c_{au}^i (q^i - q_0^i), 0\}. \quad (1.7)$$

Currently we do not use an autoconversion threshold value for cloud ice (hence,  $q_0^i = 0$ ). The rate coefficient is set to  $c_{au}^i = 10^{-3} \text{ s}^{-1}$ . We assume a monodispers size distribution for cloud ice with a mean crystal mass given by

$$m_i = \rho q^i N_i^{-1}, \quad (1.8)$$

where  $N_i$  is the number of cloud ice particles per unit volume of air. The number density  $N_i$  is parameterized as a function of temperature by

$$N_i(T) = N_0^i \exp\{0.2(T_0 - T)\}, \quad N_0^i = 1.0 \cdot 10^2 m^{-3}. \quad (1.9)$$

This simple approximation is based on aircraft measurements of the concentration of pristine crystals in stratiform clouds using data of Hobbs and Rangno (1985) and Meyers et al. (1992). A more physically based approach must involve a double-moment representation of cloud ice including a budget equation for the concentration of ice particles and maybe ice nuclei. Such schemes are not yet available for the ICON model.

For the autoconversion of cloud ice and the aggregation of cloud ice by snow a temperature dependent sticking efficiency has been introduced similar to Lin et al. (1983):

$$e_i(T) = \max(0.2, \min(\exp(0.09(T - T_0)), 1.0))$$

with  $T_0 = 273.15 \text{ K}$ .

Note that depositional growth is explicitly parameterized, thus the model predicts ice supersaturation. The change of the cloud ice mixing ratio by deposition is given by

$$\left. \frac{\partial q_i}{\partial t} \right|_{\text{dep}} = \frac{4D_v}{1 + H} \left( \frac{m_i}{a_m} \right)^{1/3} N_i (q_v - q_{i,sat}) \quad (1.10)$$

where  $H$  is the so-called Howell factor (see Doms et al. 2004 for details).

# Chapter 2

## Convection

### 1. Introduction

Cumulus convection is parametrized by a bulk mass flux scheme which was originally described in ?. The scheme considers deep, shallow and mid-level convection. Clouds are represented by a single pair of entraining/detraining plumes which describes updraught and downdraught processes. Momentum and tracer transport is also included.

### 2. Large-scale budget equations

The contributions from cumulus convection to the large-scale budget equations of heat moisture, momentum, and chemical tracers are

$$\left. \begin{aligned}
 \left( \frac{\partial \bar{s}}{\partial t} \right)_{\text{cu}} &= g \frac{\partial}{\partial p} [M_{\text{up}} s_{\text{up}} + M_{\text{down}} s_{\text{down}} - (M_{\text{up}} + M_{\text{down}}) \bar{s}] \\
 &\quad + L(c_{\text{up}} - e_{\text{down}} - e_{\text{subcld}}) - (L_{\text{subl}} - L_{\text{vap}})(M_{\text{elt}} - F_{\text{rez}}) \\
 \left( \frac{\partial \bar{q}}{\partial t} \right)_{\text{cu}} &= g \frac{\partial}{\partial p} [M_{\text{up}} q_{\text{up}} + M_{\text{down}} q_{\text{down}} - (M_{\text{up}} + M_{\text{down}}) \bar{q}] \\
 &\quad - (c_{\text{up}} - e_{\text{down}} - e_{\text{subcld}}) \\
 \left( \frac{\partial \bar{u}}{\partial t} \right)_{\text{cu}} &= g \frac{\partial}{\partial p} [M_{\text{up}} u_{\text{up}} + M_{\text{down}} u_{\text{down}} - (M_{\text{up}} + M_{\text{down}}) \bar{u}] \\
 \left( \frac{\partial \bar{v}}{\partial t} \right)_{\text{cu}} &= g \frac{\partial}{\partial p} [M_{\text{up}} v_{\text{up}} + M_{\text{down}} v_{\text{down}} - (M_{\text{up}} + M_{\text{down}}) \bar{v}] \\
 \left( \frac{\partial \bar{C}^i}{\partial t} \right)_{\text{cu}} &= g \frac{\partial}{\partial p} [M_{\text{up}} C_{\text{up}}^i + M_{\text{down}} C_{\text{down}}^i - (M_{\text{up}} + M_{\text{down}}) \bar{C}^i]
 \end{aligned} \right\} \quad (2.1)$$

where  $M_{\text{up}}$ ,  $M_{\text{down}}$  are the net contributions from all clouds to the updraught and downdraught mass fluxes,  $c_{\text{up}}$  and  $e_{\text{down}}$  are the condensation/sublimation in the updraughts, and the evaporation in the downdraughts.  $s_{\text{up}}$ ,  $s_{\text{down}}$ ,  $q_{\text{up}}$ ,  $q_{\text{down}}$ ,  $u_{\text{up}}$ ,  $u_{\text{down}}$ ,  $v_{\text{up}}$ ,  $v_{\text{down}}$ ,  $C_{\text{up}}^i$  and  $C_{\text{down}}^i$  are the weighted averages of the dry static energy  $\bar{s}$ , the specific humidity  $\bar{q}$ , the horizontal wind components  $\bar{u}$  and  $\bar{v}$  and the passive chemical tracer  $\bar{C}^i$  from all updraughts and downdraughts within a grid box (although individual convective elements are not considered) obtained from the bulk cloud model described below.  $L_{\text{subl}}$  and  $L_{\text{vap}}$  are latent heats of sublimation and vaporization, and  $L$  is the effective latent heat

for an ice–water mix (an empirical function of temperature).  $e_{\text{subclcd}}$  is the evaporation of precipitation in the unsaturated sub-cloud layer,  $M_{\text{elt}}$  is the melting rate of snow and  $F_{\text{rez}}$  is the freezing rate of condensate in the convective updraught. In addition to (2.1) the precipitation fluxes are defined as

$$P^{\text{rain}}(p) = \int_{P_{\text{top}}}^p (G^{\text{rain}} - e_{\text{down}}^{\text{rain}} - e_{\text{subclcd}}^{\text{rain}} + M_{\text{elt}}) \frac{dp}{g}; \quad P^{\text{snow}}(p) = \int_{P_{\text{top}}}^p (G^{\text{snow}} - e_{\text{down}}^{\text{snow}} - e_{\text{subclcd}}^{\text{snow}} - M_{\text{elt}}) \frac{dp}{g} \quad (2.2)$$

where  $P^{\text{rain}}$  and  $P^{\text{snow}}$  are the fluxes of precipitation in the forms of rain and snow at level  $p$ .  $G^{\text{rain}}$  and  $G^{\text{snow}}$  are the conversion rates from cloud water into rain and cloud ice into snow, and  $M_{\text{elt}}$  denotes melted precipitation. The evaporation of precipitation in the downdraughts  $e_{\text{down}}$ , and below cloud base  $e_{\text{subclcd}}$ , have been split into water and ice components,  $e_{\text{down}}^{\text{rain}}$ ,  $e_{\text{down}}^{\text{snow}}$ ,  $e_{\text{subclcd}}^{\text{rain}}$ , and  $e_{\text{subclcd}}^{\text{snow}}$ . The microphysical terms in (2.1) and (2.2) referring to the updraught are explained in detail in Section 6., those referring to the downdraught are defined in (2.17).

### 3. Cloud model equations

#### a. Updraughts

The updraught of the cloud ensemble is assumed to be in a steady state. Then the bulk equations for mass, heat, moisture, cloud water content, momentum and tracers are

$$\left. \begin{aligned} -g \frac{\partial M_{\text{up}}}{\partial p} &= E_{\text{up}} - D_{\text{up}} \\ -g \frac{\partial (M_{\text{up}} s_{\text{up}})}{\partial p} &= E_{\text{up}} \bar{s} - D_{\text{up}} s_{\text{up}} + L c_{\text{up}}, & -g \frac{\partial (M_{\text{up}} q_{\text{up}})}{\partial p} &= E_{\text{up}} \bar{q} - D_{\text{up}} q_{\text{up}} - c_{\text{up}} \\ -g \frac{\partial (M_{\text{up}} l_{\text{up}})}{\partial p} &= -D_{\text{up}} l_{\text{up}} + c_{\text{up}} - G, & -g \frac{\partial (M_{\text{up}} r_{\text{up}})}{\partial p} &= -D_{\text{up}} r_{\text{up}} + G - S_{\text{fallout}} \\ -g \frac{\partial (M_{\text{up}} u_{\text{up}})}{\partial p} &= E_{\text{up}} \bar{u} - D_{\text{up}} u_{\text{up}}, & -g \frac{\partial (M_{\text{up}} v_{\text{up}})}{\partial p} &= E_{\text{up}} \bar{v} - D_{\text{up}} v_{\text{up}} \\ -g \frac{\partial (M_{\text{up}} C_{\text{up}}^i)}{\partial p} &= E_{\text{up}} \bar{C}^i - D_{\text{up}} C_{\text{up}}^i \end{aligned} \right\} \quad (2.3)$$

where  $E_{\text{up}}$  and  $D_{\text{up}}$  are the rates of mass entrainment and detrainment,  $l_{\text{up}}$  is the updraught cloud water/ice content, and  $r_{\text{up}}$  is precipitating rain and snow. The vertical integration of (2.3) requires knowledge of the cloud-base mass flux and of the mass entrainment and detrainment rates. the cloud-base mass flux is determined for the various types of convection from the closure assumptions discussed in Section 4..

Entrainment of mass into convective plumes is assumed to occur (1) through turbulent exchange or inflow of mass through the cloud edges; and detrainment is assumed to occur (1) through turbulent exchange and (2) through organized outflow at cloud top. The superscripts (1) and (2) are used to denote the different components of the entrainment and detrainment processes

$$E_{\text{up}} = E_{\text{up}}^{(1)}, \quad D_{\text{up}} = D_{\text{up}}^{(1)} + D_{\text{up}}^{(2)} \quad (2.4)$$

*Entrainment rates* Entrainment rates ( $\text{s}^{-1}$ ) are parametrized as

$$E_{\text{up}}^{(1)} = \varepsilon_{\text{up}}^{(1)} \frac{M_{\text{up}}}{\bar{\rho}} f_{\text{scale}}^{(1)} \quad (2.5)$$

where the fractional entrainment ( $\text{m}^{-1}$ ) traditionally inversely depends on cloud radius ( $R_{\text{up}}$ ) following (Simpson and Wiggert 1969; Simpson 1971), i.e.

$$\varepsilon_{\text{up}}^{(1)} = \frac{0.2}{R_{\text{up}}} \quad (2.6)$$

With Cy36r4 the updraught entrainment formulation has been simplified to retain only one entrainment process/formulation englobing both "turbulent" and "organized" mass exchanges. Entrainment above cloud base is applied to positively buoyant convection only. Observations show that mid-tropospheric relative humidity strongly controls the cloud top heights, and it could be even shown through cloud resolving simulations (Stirling and Derbyshire, private communication) that dry environments lead to larger entrainment, probably through evaporative cooling and inflow effects. The simplest way to represent this sensitivity and to increase the mass fluxes in unstable buoyant situations, is a formulation depending on the environmental relative humidity  $RH$

$$E_{\text{up}}^{(1)} = \varepsilon_{\text{up}}^{(1)} \frac{M_{\text{up}}}{\bar{\rho}} \left( 1.3 - RH \right) f_{\text{scale}}^{(1)}, \quad \varepsilon_{\text{up}}^{(1)} = 1.8 \times 10^{-3} \text{m}^{-1}, \quad f_{\text{scale}}^{(1)} = \left( \frac{q_{\text{sat}}(\bar{T})}{q_{\text{sat}}(\bar{T}_{\text{base}})} \right)^3 \quad (2.7)$$

This entrainment formulation is able to reasonably represent the tropical variability of convection (Bechtold et al. 2008). It is applied to all types of convection, i.e. deep, shallow and mid-level, with the sole difference that for shallow and mid-level convection the entrainment rates are increased by a factor of two as compared to the deep values given by 2.7. The vertical scaling function  $f_{\text{scale}}^{(1)}$  in (2.7) is supposed to mimick the effects of a cloud ensemble and/or the effect of increasing ( $R_{\text{up}}$ ) with height. As the scaling function strongly decreases with height the detrainment rate will become eventually larger than the entrainment rate, and the mass flux starts to decrease with height. Together with the detrainment (see below) the formulation produces on average a vertical distribution of the convective mass flux that broadly follows that of the large-scale ascent which is partly supported by diagnostic studies for tropical convection (e.g. Cheng et al. 1980; Johnson 1980). Finally, note that in cycles prior to 32r3 the "organized" entrainment has been linked to the the large-scale moisture convergence as first advocated by Lindzen (1981). However, the imposed strong coupling between the large-scale and the convection had a detrimental effect on the forecasts ability to represent tropical variability. Only since Cy32r3, using entrainment rates scaled by a vertical function together with a relative humidity based organized entrainment, and a variable convective adjustment time-scale (see below), the model is able to maintain a realistic level of tropical variability.

*Detrainment rates* Turbulent detrainment rates ( $\text{s}^{-1}$ ) are parametrized as

$$D_{\text{up}}^{(1)} = \delta_{\text{up}}^{(1)} \frac{M_{\text{up}}}{\bar{\rho}} \quad (2.8)$$

with

$$\delta_{\text{up}}^{(1)} = 0.75 \times 10^{-4} \text{m}^{-1} \quad (2.9)$$

Organized detrainment is estimated from the vertical variation of the updraught vertical velocity  $w_{\text{up}}$ , which is estimated from the budget equation for the updraught kinetic energy written in height coordinates

$$\frac{\partial K_{\text{up}}}{\partial z} = -\frac{\mu_{\text{up}}}{M_{\text{up}}} (1 + \beta C_d) 2K_{\text{up}} + \frac{1}{f(1 + \gamma)} g \frac{T_{v,\text{up}} - \bar{T}_v}{\bar{T}_v} \quad (2.10)$$

with

$$K_{\text{up}} = \frac{w_{\text{up}}^2}{2} \quad (2.11)$$

where  $K_{\text{up}}$  is the updraught kinetic energy,  $T_{\text{v,up}}$  is the virtual temperature of the updraught and  $\bar{T}_{\text{v}}$  the virtual temperature of the environment.  $\mu_{\text{up}}$  is a mixing coefficient which is equal to the entrainment rate ( $E_{\text{up}}$ ), or the detrainment rate ( $D_{\text{up}}$ ) if this is larger. As entrainment is set to zero in the upper part of the cloud layer, use of detrainment in this region better represents the effect of mixing and vertical pressure gradients in the upper part of deep convective clouds, reducing vertical velocity and reducing overshoot of convective towers into the lower stratosphere.

$\gamma = 0.5$  is the virtual mass coefficient (Simpson and Wiggert 1969), the factor  $f = 2$  is introduced because the flow is highly turbulent (Cheng et al. 1980) and for the drag coefficient a value of  $C_d = 0.506$  is used (Simpson and Wiggert 1969). The value for  $\beta$  is 1.875. The cloud base value of the updraught velocity is chosen as  $1 \text{ m s}^{-1}$ .

$w_{\text{up}}$  enters the scheme in several ways: (i) for the generation and fallout of rain (Section 6.), (ii) to determine the penetration above the zero-buoyancy level and the top of cumulus updraughts (where  $w_{\text{up}}$  reduces to zero), and (iii) to specify detrainment below the top of the updraught.

Organized detrainment is estimated by equating the decrease in updraught vertical velocity due to negative buoyancy at the top of the cloud to the decrease in mass flux with height:

$$\frac{M_{\text{up}}(z)}{M_{\text{up}}(z + \Delta z)} = \sqrt{\frac{K_{\text{up}}(z)}{K_{\text{up}}(z + \Delta z)}} \quad (2.12)$$

This assumes that the cloud area remains constant in the detraining layer. (2.12) defines the reduction of mass flux with height, which combined with the updraught continuity equation (see (2.3)) gives the organised detrainment rate.

### *b. Downdraughts*

Downdraughts are considered to be associated with convective precipitation from the updraughts and originate from cloud air influenced by the injection of environmental air. Following Fritsch and Chappell (1980) and Foster (1958), the Level of Free Sinking (LFS) is assumed to be the highest model level (below the level of minimum moist static energy) where a mixture of equal parts of cloud and saturated environmental air at the wet-bulb temperature becomes negative buoyant with respect to the environmental air. The downdraught mass flux is assumed to be directly proportional to the upward mass flux. Following Johnson (1976, 1980) the mass flux at the LFS is specified from the updraught mass flux at cloud base as

$$(M_{\text{down}})_{\text{LFS}} = -\eta(M_{\text{up}})_{\text{base}} \quad \text{with} \quad \eta = 0.35 \quad (2.13)$$

The vertical distribution of the downdraught mass flux, dry static energy, moisture, horizontal momentum and passive tracers below the LFS are determined by entraining/detraining plume equations

similar to those for the updraught:

$$\left. \begin{aligned} g \frac{\partial M_{\text{down}}}{\partial p} &= E_{\text{down}} - D_{\text{down}} \\ g \frac{\partial (M_{\text{down}} s_{\text{down}})}{\partial p} &= E_{\text{down}} \bar{s} - D_{\text{down}} s_{\text{down}} + L e_{\text{down}} \\ g \frac{\partial (M_{\text{down}} q_{\text{down}})}{\partial p} &= E_{\text{down}} \bar{q} - D_{\text{down}} q_{\text{down}} - e_{\text{down}} \\ g \frac{\partial (M_{\text{down}} u_{\text{down}})}{\partial p} &= E_{\text{down}} \bar{u} - D_{\text{down}} u_{\text{down}} \\ g \frac{\partial (M_{\text{down}} v_{\text{down}})}{\partial p} &= E_{\text{down}} \bar{v} - D_{\text{down}} v_{\text{down}} \\ g \frac{\partial (M_{\text{down}} C_{\text{down}}^i)}{\partial p} &= E_{\text{down}} \bar{C}^i - D_{\text{down}} C_{\text{down}}^i \end{aligned} \right\} \quad (2.14)$$

$e_{\text{down}}$  is the evaporation of convective rain to maintain a saturated descent; the moistening and cooling of the environmental air injected at the LFS is also due to evaporating rain.

Entrainment and detrainment in downdraughts are highly uncertain as relevant data are not available. As for the updraught, both turbulent and organized entrainment/detrainment are considered.

*Turbulent entrainment and detrainment* For turbulent mixing

$$\varepsilon_{\text{down}}^{(1)} = \delta_{\text{down}}^{(1)} = 2 \times 10^{-4} \text{ m}^{-1} \quad (2.15)$$

*Organized entrainment and detrainment* Organized entrainment for the downdraught is based upon a formulation suggested by Nordeng (1994) so that

$$\varepsilon_{\text{down}}^{(2)} = \frac{\left\{ g \frac{T_{v,\text{down}} - T_{\text{down}} r_{\text{down}} - \bar{T}_v}{T_v} \right\}}{(w_{\text{down}}^{\text{LFS}})^2 - \int_{z_{\text{LFS}}}^z \left\{ g \frac{T_{v,\text{down}} - T_{\text{down}} r_{\text{down}} - \bar{T}_v}{T_v} \right\} dz} \quad (2.16)$$

where  $w_{\text{down}}^{\text{LFS}}$  is the vertical velocity in the downdraught at the LFS (set to  $-1 \text{ ms}^{-1}$ ). The total evaporation rate in the downdraft corresponds to the total downdraft precipitation rate that is simply given as

$$\sum_{k=\text{LFS}}^{\text{nlev}} e_{\text{down}} = \sum_{k=\text{LFS}}^{\text{nlev}} \frac{g}{\Delta p} (q_{\text{down},k} - \hat{q}_{\text{down},k}) M_{\text{down},k} \quad (2.17)$$

where  $q_{\text{down},k}$  is the value of the downdraft humidity computed from (2.14) without saturation adjustment, and  $\hat{q}_{\text{down},k}$  is the humidity after the saturation adjustment. The value of the rain water content in the downdraft used in (2.16) is estimated as  $r_{\text{down}} = e_{\text{down}} g / (\Delta p M_{\text{up}})$ , for the definition of the pressure thickness  $\Delta p$  of layer  $k$  see (??).

Organized detrainment from the downdraught occurs when either the downdraught becomes positively buoyant or approaches the surface. If the downdraught remains negatively buoyant until it reaches the surface then the mass flux is decreased linearly over the lowest 60 hPa of the atmosphere. However, if a downdraught becomes positively buoyant during its descent, it is detrained over one level, except where this occurs at cloud base. In this case the downdraught fluxes are decreased linearly (deep convection) or quadratically (mid-level convection) to zero at the surface.

## 4. Convection initiation and convective types

The first important task of a convection parameterization is to decide if convection is active or not in a model grid column. This is done in a very simplified “first-guess” updraught computation that implies the determination of the cloud base level, i.e. the Lifting Condensation Level (LCL), and of the properties of the cloud (updraught) at cloud base. Furthermore, in using a bulk mass flux scheme, as opposed to a scheme which considers an ensemble of convective clouds (such as that of Arakawa and Schubert 1974), some determination of convective cloud type must be made so that appropriate choices can be made for the cloud properties.

The scheme first tests for the occurrence of shallow convection by computing the ascent of a surface parcel. The following simplified updraught equation is applied

$$\frac{\partial \phi_{\text{up}}}{\partial z} = \varepsilon_{\text{up}}^{\text{ini}} (\bar{\phi} - \phi_{\text{up}}) \quad (2.18)$$

where  $\phi$  stands either for the dry static energy or the total water specific humidity. As proposed by Jakob and Siebesma (2003) the entrainment rate for the test parcel for shallow convection is set to  $\varepsilon_{\text{up}}^{\text{ini}} = 0.5 \left( \frac{0.55}{z} + 1 \times 10^{-4} \right)$ . Additionally, a temperature  $\Delta T_{\text{up}}$  and moisture excess  $\Delta q_{\text{up}}$  with respect to the environment is given to the test parcel at the lowest model level depending on the surface sensible and latent turbulent heat fluxes

$$\Delta T_{\text{up}}^{\text{shal}} = -1.5 \frac{J_s}{\rho c_p w_*} \quad \text{and} \quad \Delta q_{\text{up}}^{\text{shal}} = -1.5 \frac{J_q}{\rho L w_*} \quad (2.19)$$

where the convective-scale velocity  $w_*$  is given as

$$w_* = 1.2 \left( u_*^3 - 1.5 \frac{gz\kappa}{\bar{\rho T}} \left[ \frac{J_s}{c_p} + 0.61 \bar{T} \frac{J_v}{L} \right] \right)^{\frac{1}{3}} \quad (2.20)$$

with  $\kappa = 0.4$  the von Kármán constant; the friction velocity  $u_*$  is set to a constant value of  $0.1 \text{ ms}^{-1}$ . The convective-scale velocity  $w_*$  is also used to initialise the updraught vertical velocity at the first model level. A grid column is then identified as shallow convective if a LCL is found for the surface parcel, if the updraught vertical velocity at the LCL (obtained by solving the kinetic energy equation (2.10)) is positive, and if the cloud thickness is smaller than 200 hPa.

Next, the occurrence of deep convection is tested for by repeating the updraught computations but starting at the next higher model level. However, the entrainment rate is now set as for the first full updraught computation (??), i.e.  $\varepsilon_{\text{up}}^{\text{ini}} = \varepsilon_{\text{up}}^{(1)}$ , simplified microphysics is taken into account by removing at each level 50% of the condensed water; the initial parcel perturbations are specified as

$$\Delta T_{\text{up}}^{\text{deep}} = 0.2 \text{ K} \quad \text{and} \quad \Delta q_{\text{up}}^{\text{deep}} = 1 \times 10^{-4} \text{ kg kg}^{-1} \quad (2.21)$$

and the updraught vertical velocity at the departure level is initialised to  $1 \text{ ms}^{-1}$ . Furthermore, in the lowest 60 hPa of the atmosphere that typically correspond to the mixed-layer depth over oceanic regions, the updraught values of the dry static energy (or humidity) at the departure level  $k$  are initialised as  $s_{\text{up},k} = \tilde{s}_k + c_p \Delta T_{\text{up}}^{\text{deep}}$ , where the tilde symbol represents a 50 hPa layer average, instead of  $s_{\text{up},k} = \bar{s}_k + c_p \Delta T_{\text{up}}^{\text{deep}}$  as for departure levels above the assumed 60 hPa mixed-layer. The idea behind is that deep convection requires a sufficiently deep source layer, this procedure also avoids spurious convection in the early morning hours when the surface-layer undergoes strong heating. A grid-column is then identified as deep-convective, if a LCL is found and the resulting cloud (the top being defined as the level where the updraught vertical velocity vanishes) is thicker

than 200 hPa. If this criterion is verified the cloud is identified as deep and the results obtained for the shallow convective test parcel are ignored (only one cloud type can exist). If no deep convective cloud is found for the given departure level, the procedure is repeated starting from the next higher model level and so on until the departure level of the test parcel is more than 350 hPa above ground. A summary of this procedure, and a discussion of the consequences for the simulation of the diurnal cycle of convection over land is given in Bechtold et al. (2004).

Finally, if neither deep nor shallow convection has been found, elevated (or mid-level) convection is tested for (see Subsection c.). Also, at the end of this procedure and if a column has been identified as convective, the computed values of the updraught vertical velocity, dry static energy, liquid water and specific humidity at cloud base are used to initialise the following full updraught computation at cloud base. The updraught values of the horizontal wind components at cloud base are simply set to the environmental values at the level just below (see Section 9.).

In the following, the determination of the convective activity (as controlled by the cloud-base mass flux) is discussed separately for each type of convection.

#### a. Deep convection

Following Fritsch and Chappell (1980) and Nordeng (1994), the cloud base mass flux for deep convection is estimated from assuming that convection acts to reduce the convective available potential energy (CAPE) towards zero over a specified time scale  $\tau$ . Therefore

$$\frac{\partial \text{CAPE}}{\partial t} = -\frac{\text{CAPE}}{\tau} = \int_{z_{\text{base}}}^{z_{\text{top}}} \frac{g}{\bar{T}_v} \left( \frac{\partial \bar{T}_v}{\partial t} \right)^{\text{cum}} dz \approx \int_{z_{\text{base}}}^{z_{\text{top}}} \frac{M_{\text{cld}}}{\bar{\rho}} \frac{g}{\bar{T}_v} \left( \frac{\partial \bar{T}_v}{\partial z} \right) dz \quad (2.22)$$

where

$$M_{\text{cld}} = M_{\text{up}} + M_{\text{down}} = \alpha[M_{\text{up}}]_{\text{base}} + \beta[M_{\text{down}}]_{\text{LFS}} \quad (2.23)$$

where  $\alpha$  and  $\beta$  describe the vertical variation of the updraught and downdraught mass flux due to entrainment and detrainment and the subscript ‘base’ refers to cloud-base quantities. As the downdraught mass flux at the LFS is linked to the updraught mass flux at cloud base (see (2.13)) then

$$M_{\text{cld}} = [M_{\text{up}}]_{\text{base}}(\alpha - \beta\eta) \quad (2.24)$$

Using (2.24) in (2.22) results in an expression for the ‘final’ cloud base mass flux given by

$$[M_{\text{up}}]_{\text{base}} = \frac{\frac{\text{CAPE}}{\tau}}{g \int_{z_{\text{base}}}^{z_{\text{top}}} (\alpha - \beta\eta) \frac{g}{\bar{\rho} \bar{T}_v} \frac{\partial \bar{T}_v}{\partial z} dz} = \frac{\frac{\text{CAPE}}{\tau}}{g \int_{z_{\text{base}}}^{z_{\text{top}}} \frac{M_{\text{cld}}^{n-1}}{M_{\text{base}}^{n-1}} \frac{1}{\bar{\rho} \bar{T}_v} \frac{\partial \bar{T}_v}{\partial z} dz} \quad (2.25)$$

where  $M_{\text{cld}}^{n-1}$  is the cloud mass flux from the first full updraught ( $n - 1 = 1$ ) computation that has been initialised with a unit cloud base mass flux  $M_{\text{base}}^{n-1} = 0.1 \Delta p_{\text{base}} / (g \Delta t)$ , with  $\Delta t$  the model time step, and where CAPE is estimated from the parcel ascent incorporating the effects of water loading,

$$\text{CAPE} = \int_{z_{\text{base}}}^{z_{\text{top}}} g \left( \frac{T_{v,\text{up}} - \bar{T}_v}{\bar{T}_v} - l_{\text{up}} \right) dz \quad (2.26)$$

Using these estimates the updraught mass flux at cloud base is recomputed and downdraught mass fluxes are rescaled. A second updraught ascent is then computed to revise the updraught properties.

The closure is complete with the specification of the adjustment time scale  $\tau$ . In cycles prior to 32r3 it was set close to or larger than the model time step ( $\tau=3600$  s at T159, 1200 s at T511 and 720 s at T799). In cycle 32r3 it is set proportional to a convective turnover time scale

$$\tau = \bar{w}_{\text{up}}^H \alpha_{n_T}, \quad \alpha_{n_T} = (1 + 264/n_T), \quad \max(720, \Delta t) \leq \tau \leq 10800 \text{ s} \quad (2.27)$$

where  $H$  is the cloud depth,  $\bar{w}_{\text{up}}^H$  is the cloud average updraught velocity, and  $\alpha_{n_T}$  is a proportionality factor depending on horizontal resolution (model truncation  $n_T$ ) so that the adjustment time scale varies by roughly a factor of two between model truncations T799 and T159. An absolute lower bound of 720 s for  $\tau$  also helps to facilitate the transition to more resolved convection at high horizontal resolutions ( $\geq$  T1279) when the model time step becomes smaller than 720 s.

### b. Shallow convection

Here we consider cumulus convection, which predominantly occurs in undisturbed flow, that is in the absence of large-scale convergent flow. Typical examples are trade-wind cumuli under a subsidence inversion, convection occurring in the ridge region of tropical easterly waves and daytime convection over land. This type of convection seems to be effectively controlled by sub-cloud layer turbulence. In fact, most of the diagnostic studies carried out for trade-wind cumuli show that the net upward moisture flux at cloud-base level is nearly equal to the turbulent moisture flux at the surface (Le Mone and Pennell 1976). In regions of cold air flowing over relatively warm oceans the strong sensible heat flux has been found to be of significant importance. We therefore derive the mass flux at cloud base on a balance assumption for the sub-cloud layer based on the moist static energy budget given by

$$[M_{\text{up}}(h_{\text{up}} - \bar{h})]_{\text{base}} = - \int_{\text{surf}}^{\text{base}} \left( \bar{\mathbf{V}} \cdot \nabla \bar{h} + \bar{\omega} \frac{\partial \bar{h}}{\partial p} - c_p \left( \frac{\partial \bar{T}}{\partial t} \right)_{\text{rad}} + \frac{\partial}{\partial p} (\overline{\omega' h'})_{\text{turb}} \right) \frac{dp}{g} \quad (2.28)$$

with

$$\bar{h} = c_p \bar{T} + L \bar{q} + gz \quad (2.29)$$

The moisture supply to the shallow cumulus is largely through surface evaporation as the contributions from large-scale convergence are either small or even negative, such as in the undisturbed trades where dry air is transported downward to lower levels.

An initial estimate for the updraught base mass flux is obtained using (2.28). If downdraughts occur (relatively rare for shallow convection due to the low precipitation rates), then a revised estimate is made accounting for the impact of downdraughts upon the sub-cloud layer, the l.h.s. of (2.28) being replaced by

$$[M_{\text{up}}(h_{\text{up}} - \bar{h})]_{\text{base}} + [M_{\text{down}}(h_{\text{down}} - \bar{h})]_{\text{base}} = [M_{\text{up}}(h_{\text{up}} - \bar{h})]_{\text{base}} - [\beta \eta M_{\text{up}}(h_{\text{down}} - \bar{h})]_{\text{base}} \quad (2.30)$$

Again downdraught properties are obtained using the original estimate of the updraught base mass flux and then rescaled by the revised value. For the updraught a second ascent is calculated using the revised value of the base mass flux.

No organized entrainment is applied to shallow convection. As turbulent entrainment and detrainment rates are equal, the mass flux remains constant with height until reducing at cloud top by organized detrainment.

### c. Mid-level convection

Mid-level convection, that is, convective cells which have their roots not in the boundary layer but originate at levels above the boundary layer, often occur at rain bands at warm fronts and in the warm sector of extratropical cyclones (Browning et al. 1973; Houze et al. 1976; Herzegh and Hobbs 1980). These cells are probably formed by the lifting of low level air until it becomes saturated (Wexler and Atlas

1959) and the primary moisture source for the clouds is from low-level large-scale convergence (Houze et al. 1976). Often a low-level temperature inversion exists that inhibits convection from starting freely from the surface; therefore convection seems to be initiated by lifting low-level air dynamically to the level of free convection. This occurs often in connection with mesoscale circulations which might be related to conditionally symmetric instability (Bennets and Hoskins 1979; Bennets and Sharp 1982) or a wave-CISK mechanism (Emanuel 1982).

Although it is not clear how significant the organization of convection in mesoscale rain bands is for the large-scale flow, a parametrization should ideally account for both convective and mesoscale circulations. Such a parametrization, however, is presently not available and we must therefore rely on simplified schemes. Here we use a parametrization which in a simple way considers the finding of the diagnostic studies mentioned above. We assume that mid-level convection can be activated in a height range between  $5 \times 10^2 \text{ m} < z < 1 \times 10^4 \text{ m}$  when there is a large-scale ascent, and the environmental air is sufficiently moist, i.e. of relative humidity in excess of 80%.

The convective mass flux at cloud base is set equal to the vertical mass transport by the large-scale flow at that level:

$$\bar{\rho}_{\text{base}} \bar{w}_{\text{base}} = (M_{\text{up}})_{\text{base}} + (M_{\text{down}})_{\text{base}} = (M_{\text{up}})_{\text{base}} (1 - \beta \eta) \quad (2.31)$$

following the notation of Subsection a. above. Again two estimates of the updraught base mass flux are made; first neglecting downdraughts, followed by a revised estimate if downdraughts occur. The closure ensures that the amount of moisture which is vertically advected through cloud base by the large-scale ascent is fully available for generation of convective cells.

## 5. Sub-cloud layer

The first level at which convective mass, momentum and thermodynamic fluxes are estimated is cloud base. To represent the effects of convective updraughts on the sub-cloud layer a simple scaling of cloud base fluxes is applied in which they decrease to zero at the surface through the sub-cloud layer.

Care must be taken to ensure that fluxes of liquid water are zero below cloud base. Through the cloud base level an interpolation of the fluxes of liquid water static energy and total water content is used to estimate fluxes of dry static energy and water vapour mixing ratio in the level immediately below cloud base;

$$\begin{aligned} (Ms)_{\text{up}}^{\text{base}+1} &= (Z^n)(Ms)_{\text{up}}^{\text{base}} - L(Ml)_{\text{up}}^{\text{base}} \\ (Mq)_{\text{up}}^{\text{base}+1} &= (Z^n)(Mq)_{\text{up}}^{\text{base}} + (Ml)_{\text{up}}^{\text{base}} \\ (Ml)_{\text{up}}^{\text{base}+1} &= 0 \end{aligned} \quad (2.32)$$

where  $\phi^{\text{base}+1}$  refers to the value of  $\phi$  at the level immediately below cloud base.  $Z$  is given by

$$Z = \left( \frac{p_{\text{surf}} - p_{\text{base}+1}}{p_{\text{surf}} - p_{\text{base}}} \right)^m \quad (2.33)$$

and  $p_{\text{surf}}$  is the surface pressure.

For deep and shallow convection  $m$  is set to 1 (implying a linear decrease in the flux with pressure below cloud base) while for mid-level convection  $m$  is equal to 2 (implying a quadratic reduction in flux below cloud base).

For the remainder of the sub-cloud layer, fluxes at level ‘B + 1’ are reduced to zero at the surface using  $Z$  recomputed as

$$Z = \left( \frac{p_{\text{surf}} - p_k}{p_{\text{surf}} - p_{\text{base}+1}} \right)^m \quad (2.34)$$

where  $p_k$  is the pressure at level model  $k$ .

The cloud-mass and momentum fluxes in the sub-cloud layer are treated in a similar manner.

## 6. Cloud microphysics

### a. Condensation rate in updraughts

The updraught condensation rate  $c_{\text{up}}$  is computed through a saturation adjustment

$$c_{\text{up}} = \frac{g}{\Delta p} (q_{\text{up}} - \hat{q}_{\text{up}}) M_{\text{up}} \quad (2.35)$$

where  $q_{\text{up}}$  is the value of the specific humidity before the saturation adjustment, and  $\hat{q}_{\text{up}}$  is the specific humidity at saturation after the adjustment.

### b. Freezing in convective updraughts

We assume that condensate in the convective updraughts freezes in the temperature range  $250.16 \text{ K} < T < 273.16 \text{ K}$  maintaining a mixed phase within that range according to (??) (see IFS model docu ‘Clouds and large-scale precipitation’).

### c. Generation of precipitation

The conversion from cloud water/ice to rain/snow is treated in a consistent way with that in the large-scale precipitation scheme by using a formulation following Sundqvist (1978)

$$G^{\text{precip}} = \frac{M_{\text{up}}}{\bar{\rho}} \frac{c_0}{0.75 w_{\text{up}}} l_{\text{up}} [1 - \exp\{-(l_{\text{up}}/l_{\text{crit}})^2\}] \quad (2.36)$$

where  $c_0 = 1.4 \times 10^{-3} \text{ s}^{-1}$  and  $l_{\text{crit}} = 0.5 \text{ g kg}^{-1}$ .  $w_{\text{up}}$  is the updraught vertical velocity and is limited to a maximum value of  $10 \text{ m s}^{-1}$  in (2.36). Conversion only proceeds if  $l_{\text{up}}$  is greater than a threshold liquid water content of  $0.3 \text{ g kg}^{-1}$  over water and  $0.5 \text{ g kg}^{-1}$  over land to prevent precipitation generation from small water contents. With this value the updraft condensate content is probably still overestimated. However, with even larger values of the conversion coefficient the precipitation efficiency of the convection scheme would be too high, and the detrainment of cloud condensate too low.

Sundqvist (1978) takes into account the Bergeron–Findeisen process for temperatures below  $-5^\circ\text{C}$  through a temperature dependent modification of  $c_0$  and  $l_{\text{crit}}$  given by

$$\begin{aligned} c'_0 &= c_0 C_{\text{BF}} \\ l'_{\text{crit}} &= l_{\text{crit}} / C_{\text{BF}} \end{aligned} \quad (2.37)$$

where

$$\begin{aligned} c_{\text{BF}} &= 1 + 0.5\sqrt{\min(T_{\text{BF}} - T_{\text{up}}, T_{\text{BF}} - T_{\text{ice}})} && \text{for } T < T_{\text{BF}} \\ c_{\text{BF}} &= 1 && \text{for } T > T_{\text{BF}} \end{aligned} \quad (2.38)$$

with  $T_{\text{BF}} = 268.16$  K and  $T_{\text{ice}} = 250.16$  K.

Equation (2.36) is integrated analytically in the vertical using the generic differential equation  $dl/dz = -al + b$ , where  $l$  is the cloud water,  $a = G^{\text{precip}}\bar{\rho}/(l_{\text{up}}M_{\text{up}})$ , and  $b = c_{\text{up}}\Delta t$ . The analytical solution is then given by  $l = l_0\exp^{-az} + b/a(1 - \exp^{-az})$ .

#### d. Fallout of precipitation

The fallout of rain water/snow is parametrized as (e.g. Kuo and Raymond 1980)

$$S_{\text{fallout}} = \frac{g}{\Delta p} M_{\text{up}} \frac{V}{w_{\text{up}}} r_{\text{up}} \quad (2.39)$$

where  $\Delta p$  is the model layer depth. The terminal velocity  $V$  is parametrized as (Liu and Orville 1969)

$$V = 21.18r_{\text{up}}^{0.2} \quad (2.40)$$

Since the fall speed of ice particles is smaller than that of water droplets, only half the value of  $V$  calculated with (2.40) is used for ice. In estimating the fallout of precipitation in the mixed phase region of the cloud a weighted mean of the fall speed for ice and water precipitation is used. Equation (2.39) is integrated in the vertical with the same analytical framework as(2.36).

#### e. Evaporation of rain

The evaporation rate of convective rain below cloud base is activated when the relative humidity  $RH$  in the environment drops below 90% over water and 70% over land. It is parametrized following Kessler (1969), where the evaporation is assumed to be proportional to the saturation deficit  $(\bar{q}_{\text{sat}} - \bar{q})$  and to be dependent on the density of rain  $\rho_{\text{rain}}$  ( $\text{gm}^{-3}$ )

$$e_{\text{subcld}} = \alpha_1 (RH\bar{q}_{\text{sat}} - \bar{q}) \rho_{\text{rain}}^{13/20} \quad (2.41)$$

where  $\alpha_1$  is a constant being zero for  $\bar{q} > RH\bar{q}_{\text{sat}}$ .

As the density of rain  $\rho_{\text{rain}}$  is not given by the model it is convenient to express it in terms of the precipitation flux  $P$  ( $\text{kg m}^{-2} \text{s}^{-1}$ ) as

$$P = \rho_{\text{rain}} V_{\text{rain}} \quad (2.42)$$

where  $V_{\text{rain}}$  is the mean fall speed of rain drops which again is parametrized following Kessler (1969).

$$V_{\text{rain}} = \alpha_2 \rho_{\text{rain}}^{1/8} / \sqrt{p/p_{\text{surf}}} \quad (2.43)$$

(Note that this is different from the formulation used in the estimation of the fallout of precipitation.)

Considering that the convective rain takes place only over a fraction  $C_{\text{conv}}$  of the grid area, the evaporation rate at level  $k$  becomes

$$e_{\text{subcld}} = C_{\text{conv}} \alpha_1 (RH\bar{q}_{\text{sat}} - \bar{q}) \left[ \frac{\sqrt{p/p_{\text{surf}}}}{\alpha_2} \frac{P}{C_{\text{conv}}} \right]^{\alpha_3} \quad (2.44)$$

where the constants have the following values (Kessler 1969)

$$\alpha_1 = 5.44 \times 10^{-4} \text{ s}^{-1} \quad \alpha_2 = 5.09 \times 10^{-3} \quad \alpha_3 = 0.57777$$

and where for the fractional area of precipitating clouds a constant value of  $C_{\text{conv}} = 0.05$  is assumed.

#### *f. Melting and freezing of precipitation*

Melting of snow falling across the freezing level  $T_0$  is parameterized by a simple relaxation towards  $T_0$  so that

$$M_{\text{elt}} = \frac{c_p (\bar{T} - T_0)}{L_f \tau} \Delta p \quad (2.45)$$

where  $M_{\text{elt}}$  is the rate of melting and  $\tau_{\text{melt}}$  is a relaxation time scale which decreases with increasing temperature

$$\tau_{\text{melt}} = \frac{\tau_m}{\{1 + 0.5(\bar{T} - \bar{T}_0)\}} \quad (2.46)$$

where  $\tau_m = 11800$  s. The parametrization may produce melting over a deeper layer than observed (Mason 1971) but this has been intentionally introduced to account implicitly for the effects of vertical mixing which may develop in response to the production of negative buoyancy.

## 7. Link to cloud scheme

Before the introduction of the prognostic cloud scheme (see IFS model docu‘Clouds and large-scale precipitation’) water detrained from convection ( $D_{\text{up}} l_{\text{up}}$ ) was evaporated instantaneously. However with the prognostic cloud scheme water detrained from convection is a source of cloud mass increasing the cloud fraction and water content of clouds. Therefore

$$\begin{aligned} \frac{\partial a}{\partial t} &= D_{\text{up}} l_{\text{up}} \\ \frac{\partial \bar{l}}{\partial t} &= D_{\text{up}} l_{\text{up}} \end{aligned} \quad (2.47)$$

where  $a$  is the cloud fraction and  $\bar{l}$  the grid-box mean cloud water.

## 8. Momentum transport and kinetic energy dissipation

Equation set (2.3) includes a treatment of the vertical transport of horizontal momentum by convection. Studies have shown that for deep convection momentum transports are overestimated by the plume models unless the effects of cloud scale horizontal pressure gradients are included (Gregory et al. 1997). For unorganised convection the effects of the pressure gradients are to adjust the in-cloud winds towards those of the large-scale flow. This can be represented by an enhanced turbulent entrainment rate in the cloud momentum equations. To ensure mass continuity the turbulent detrainment rate is also increased by an equivalent amount.

Hence for deep and mid-level convection the turbulent entrainment and detrainment used in the updraught momentum equation are

$$\begin{aligned} \varepsilon_{\text{up}}^{(1),(u,v)} &= \varepsilon_{\text{up}}^{(1)} + \lambda \delta_{\text{up}}^{(1)} \\ \delta_{\text{up}}^{(1),(u,v)} &= \delta_{\text{up}}^{(1)} + \lambda \delta_{\text{up}}^{(1)} \end{aligned} \quad (2.48)$$

where  $\delta_{\text{up}}^{(1)}$  is given by (??).

For deep and mid-level convection  $\lambda = 2$ , while for shallow convection  $\lambda = 0$ . Gregory (1997) suggests that the above formulation provides an adequate description of the effects of cloud scale pressure gradients in cases of deep convection. For shallow convection and downdraughts it is assumed that the effects of the pressure gradient term can be neglected and no enhancement of the entrainment rates in the momentum equations is applied. This formulation limits the momentum transports to be downgradient. Upgradient transports by highly organized convective systems (e.g. African squall lines) are not captured by this method.

The definition of the horizontal wind in the updraught and downdraught at and below cloud base and LFS is not well known. For the updraught, the value at cloud base is set to the environmental value at the departure level. For the downdraught, the initial values at the LFS are set equal to the average values of the winds in the updraught and those of the large-scale flow. The updraught values below cloud base are derived assuming a linear decrease of the fluxes from their cloud base value to zero at the surface. Finally, in order to correct for an apparent low-bias in the near surface wind speeds with the present linear flux relation (quasi-linear in case of an implicit time discretisation see Section 10.), the updraught velocities are decreased by a constant perturbation  $u_{\text{pert}}=0.3 \text{ m s}^{-1}$

$$\begin{aligned} u_{\text{up}} &= u_{\text{up}} - u_{\text{pert}} \text{sign}(\bar{u}) \\ v_{\text{up}} &= v_{\text{up}} - u_{\text{pert}} \text{sign}(\bar{v}). \end{aligned} \quad (2.49)$$

Finally, with the introduction of Cy36r4 we have included the dissipation of the kinetic energy as a consequence of the convective momentum transport as an additional large-scale heat source as the convective momentum transport conserves momentum but not energy. The total kinetic energy dissipation  $D_{\text{st}}$  ( $\text{W m}^{-2}$ ) in a model column can be estimated as

$$D_{\text{st}} \approx - \left( \frac{\partial K}{\partial t} \right)_{\text{cu}} \approx \int_{P_{\text{surf}}}^0 \left( \bar{u} \left( \frac{\partial u}{\partial t} \right)_{\text{cu}} + \bar{v} \left( \frac{\partial v}{\partial t} \right)_{\text{cu}} \right) \frac{dp}{g} \quad (2.50)$$

A more precise formulation of the dissipation and discussion is provided in Steinheimer et al. (2007). Unfortunately one does not really know where the dissipation actually occurs. But one can reasonably distribute the dissipation over the model column using the module of the tendencies to obtain an additional convective heating due to kinetic energy dissipation as

$$\left( \frac{\partial \bar{T}}{\partial t} \right)_{\text{cu}} = c_p^{-1} D_{\text{st}} g f(p); \quad f(p) = \frac{\sqrt{\left( \frac{\partial u}{\partial t} \right)_{\text{cu}}^2 + \left( \frac{\partial v}{\partial t} \right)_{\text{cu}}^2}}{- \int_{P_{\text{surf}}}^0 \sqrt{\left( \frac{\partial u}{\partial t} \right)_{\text{cu}}^2 + \left( \frac{\partial v}{\partial t} \right)_{\text{cu}}^2} dp} \quad (2.51)$$

## 9. Vertical discretization of the model equations

The flux divergence in the large-scale budget equations (2.1) and in the cloud equations (2.3) and (2.14) are approximated by centred finite differences as

$$g \frac{\partial(M\phi)}{\partial p} = \frac{g}{\Delta p} (M_{k+1/2} \phi_{k+1/2} - M_{k-1/2} \phi_{k-1/2}), \quad \Delta p = p_{k+1/2} - p_{k-1/2} \quad (2.52)$$

Furthermore, the updraught/downdraught equations (2.3) and (2.14) including the entrainment/detrainment terms are discretized as

$$\begin{aligned} \frac{g}{\Delta p}(M_{\text{up},k-1/2}\phi_{\text{up},k-1/2} - M_{\text{up},k+1/2}\phi_{\text{up},k+1/2}) &= E_{\text{up}}\bar{\phi}_{k+1/2} - D_{\text{up}}\phi_{\text{up},k+1/2} \\ \frac{g}{\Delta p}(M_{\text{down},k+1/2}\phi_{\text{down},k+1/2} - M_{\text{down},k-1/2}\phi_{\text{down},k-1/2}) &= E_{\text{down}}\bar{\phi}_{k-1/2} - D_{\text{down}}\phi_{\text{down},k-1/2} \end{aligned} \quad (2.53)$$

The updraught equation is solved for  $\phi_{\text{up},k-1/2}$  and the downdraught equation for  $\phi_{\text{down},k+1/2}$ . Note that with the definition (2.5) the terms  $E_{\text{down}}$  and  $D_{\text{down}}$  are negative. For the horizontal wind components and for tracers, the half-level environmental values are defined as shifted full-level values, i.e.  $\bar{\phi}_{k+1/2} = \bar{\phi}_k$  and  $\bar{\phi}_{k-1/2} = \bar{\phi}_{k-1}$ . For temperature (dry static energy) and humidity, the half-level environmental values are determined by downward extrapolation from the next full level above along a cloud-ascent through that level giving

$$\left. \begin{aligned} \bar{T}_{k+1/2} &= \bar{T}_k + \left( \frac{\partial \bar{T}}{\partial p} \right)_{h_{\text{sat}}} (p_{k+1/2} - p_k) \\ \bar{q}_{k+1/2} &= \bar{q}_k + \left( \frac{\partial \bar{q}}{\partial p} \right)_{h_{\text{sat}}} (p_{k+1/2} - p_k) \end{aligned} \right\} \quad (2.54)$$

where  $h_{\text{sat}} = c_p T + gz + Lq_{\text{sat}}$  is the saturation moist static energy. Using an extrapolation like (2.54) for calculating the subsidence of environmental air assures smooth profiles, and is also more consistent with the calculation of the updraughts where cloud air is transported upwards through level  $k+1/2$  with the thermal state below that level and equally with the downdraughts which depend only on values of  $s$  and  $q$  above that level. Similarly, because of (2.54) the subsidence of environmental air through the same level accounts now only for thermal properties above that level. The choice of a moist adiabat for extrapolation is dictated by the property of the moist static energy which is, by convection in the absence of downdraughts, only changed through the fluxes of moist static energy

$$\left( \frac{\partial \bar{h}}{\partial t} \right)_{\text{cu}} = g \frac{\partial}{\partial p} [M_{\text{up}}(h_{\text{up}} - \bar{h})] \quad (2.55)$$

As the lines of the saturation moist static energy  $h_{\text{sat}}$  through point  $(p_{k+1/2}, \bar{T}_{k-1/2})$  and the updraught moist static energy are almost parallel, apart from entrainment effects, the difference  $h_{\text{up}} - \bar{h}$  is little affected by the vertical discretization.

The ascent in the updraughts is obtained by vertical integration of (2.3). Starting at the surface the condensation level (equal to the lowest half-level which is saturated or supersaturated and where updraught velocity is positive) is determined from an adiabatic ascent. The cloud profile above cloud base is determined layer by layer by first doing a dry adiabatic ascent with entrainment and detrainment included and then adjusting temperature and moisture towards a saturated state, taking into account condensation and freezing processes. The buoyancy of the parcel is calculated taking into account the effects of cloud and precipitation water loading so that

$$B = T_{\text{up}}(1 + 0.608q_{\text{up}} - l_{\text{up}} - r_{\text{up}}) - \bar{T}(1 + 0.608q_e) \quad (2.56)$$

Special care has to be taken in the discretization of (2.10) because of overshooting effects. A centred differencing scheme is used so that

$$\begin{aligned} \frac{K_{\text{up},k-1/2} - K_{\text{up},k+1/2}}{z_{k-1/2} - z_{k+1/2}} &= \frac{E_{\text{up},k}}{M_{\text{up},k+1/2}} (1 + \beta C_d) \{K_{\text{up},k-1/2} + K_{\text{up},k+1/2}\} \\ &+ \frac{1}{f(1 + \gamma)} \frac{1}{2} g \left[ \frac{\{T_{\text{v,up}} - \bar{T}_{\text{v}}\}_{k-1/2}}{\{T_{\text{v}}\}_{k-1/2}} + \frac{\{T_{\text{v,up}} - \bar{T}_{\text{v}}\}_{k+1/2}}{\{T_{\text{v}}\}_{k+1/2}} \right] \end{aligned} \quad (2.57)$$

Finally, we mention that for numerical reasons the environmental air must not be convectively unstably stratified so

$$\bar{s}_{k-1/2} \geq \bar{s}_{k+1/2} \quad (2.58)$$

In fact, one of the forecasts with the ECMWF global model became numerically unstable when (2.56) was not imposed.

## 10. Temporal discretization

The convective tendencies for the environmental values are obtained by an explicit solution of the advection equation (2.1) written in flux form

$$\left( \frac{\partial \bar{\phi}}{\partial t} \right)_{\text{cu}} = \frac{\bar{\phi}_k^{n+1} - \bar{\phi}_k^n}{\Delta t} = \frac{g}{\Delta p} [M_{\text{up}} \phi_{\text{up}} + M_{\text{down}} \phi_{\text{down}} - (M_{\text{up}} + M_{\text{down}}) \bar{\phi}^n]_{k-1/2}^{k+1/2} \quad (2.59)$$

as the tendency (or the new environmental value  $\bar{\phi}$  at time  $n + 1$ ) only depends on quantities known at time step  $n$ . However, in order for the explicit solution to be stable it must satisfy the Courant–Friedrich–Levy (CFL) criterion, and therefore the mass flux values should be limited to

$$M_{\text{up}} + M_{\text{down}} \leq \frac{\Delta p}{g \Delta t} \quad (2.60)$$

It turned out that this mass flux limit is frequently reached in the case of shallow convection and long model time steps of order  $\Delta t > 1800$  s, and that the application of this mass flux limiter contributed to a sensitivity of model results to the model time step. Therefore, from model cycle Cy26r3 onwards it was decided to relax this mass flux limiter to three times the value given by the CFL criterion in the case of shallow convection and for model time steps  $\Delta t > 1800$  s – as a further restriction this relaxed mass flux limiter is only applied to temperature and humidity, but not to the horizontal winds.

With cycle Cy31r1 onwards the convective transports are solved implicitly for chemical tracers and horizontal winds, whereas a semi-implicit formulation is used for specific humidity and dry static energy. The implicit formulation for tracers or momentum reads

$$\left( \frac{\partial \bar{\phi}}{\partial t} \right)_{\text{cu}} = \frac{\bar{\phi}_k^{n+1} - \bar{\phi}_k^n}{\Delta t} = \frac{g}{\Delta p} [M_{\text{up}} \phi_{\text{up}} + M_{\text{down}} \phi_{\text{down}} - (M_{\text{up}} + M_{\text{down}}) \bar{\phi}^{n+1}]_{k-1/2}^{k+1/2} \quad (2.61)$$

With the “shifted” vertical discretization for Tracers and horizontal winds  $\bar{\phi}_{k+1/2} = \bar{\phi}_k$  and  $\bar{\phi}_{k-1/2} = \bar{\phi}_{k-1}$ , this equation constitutes a bi-diagonal linear system with unknowns  $\bar{\phi}_k^{n+1}$  and  $\bar{\phi}_{k-1}^{n+1}$ .

However, the implicit formulation for specific humidity and dry static energy (temperature) is less straightforward, as the half-level values are non-linear functions of the full-level values (2.56). However, expressing the half-level values as a linear function of the full-level values

$$\begin{aligned} \bar{s}_{k-1/2}^{n+1} &= \bar{s}_{k-1}^{n+1} + \alpha_{k-1/2}^{(s)} \bar{s}_k^n \\ \bar{q}_{k-1/2}^{n+1} &= \bar{q}_{k-1}^{n+1} + \alpha_{k-1/2}^{(q)} q_{\text{sat}}(\bar{T}_k^n), \end{aligned} \quad (2.62)$$

with the coefficients  $\alpha^{(s)}$  and  $\alpha^{(q)}$  precomputed from

$$\begin{aligned} \bar{s}_{k-1/2}^n &= \bar{s}_{k-1}^n + \alpha_{k-1/2}^{(s)} \bar{s}_k^n \\ \bar{q}_{k-1/2}^n &= \bar{q}_{k-1}^n + \alpha_{k-1/2}^{(q)} q_{\text{sat}}(\bar{T}_k^n) \end{aligned} \quad (2.63)$$

the same bi-diagonal linear equation system as for tracers and momentum is obtained. Note that only the temperature and not the geopotential term of the dry static energy is formulated implicitly, and that the saturation specific humidity  $q_{\text{sat}}(\bar{T}_k^n)$  has been preferred to  $q_k^n$  as it is smoother and positive definite. Overall the implicit solution provides a stable solution, and smoother and non-local vertical profiles of tendencies through its inherent diffusivity. With Cy32r3 onward the mass flux CFL limit for temperature and humidity is set to 5 for horizontal resolutions below T511, and to 3 for all higher resolutions. For momentum a CFL limit of 1 is retained in order to prevent too strong surface winds.

## 11. Diagnostics for postprocessing: CAPE and CIN

As the CAPE computed in the convection routines is only computed for convectively active model columns, but taking into account lateral entrainment and liquid water loading (2.22) it was decided to provide to forecasters a CAPE product that is horizontally more homogeneous and close in line with the actual WMO definition (i.e the CAPE corresponding to a pseudo-adiabatic ascent)

$$\text{CAPE} = \int_{z_{\text{dep}}}^{z_{\text{top}}} g \left( \frac{T_{\text{up}} - \bar{T}}{\bar{T}} \right) dz \approx \int_{z_{\text{dep}}}^{z_{\text{top}}} g \left( \frac{\theta_{\text{e,up}} - \bar{\theta}_{\text{esat}}}{\bar{\theta}_{\text{esat}}} \right) dz \quad (2.64)$$

For reasons of numerical efficiency the CAPE has been approximated using the updraught equivalent potential temperature  $\theta_e = T \left( \frac{p_0}{p} \right)^{R/c_p} \exp \left( \frac{Lq}{c_p T} \right)$  which is conserved during pseudo-adiabatic ascent, and the environmental saturated  $\theta_e$  which is a function of the environmental temperature only; a more accurate formulation of  $\theta_e$  could have been used using e.g. the temperature at the LCL and taking into account glaciation processes, but the present simple definition is of sufficient accuracy for the diagnostic purpose.

The above integral is evaluated for parcels ascending from model levels in the lowest 350 hPa initialising  $\theta_{\text{e,up}} = \bar{T}_k \left( \frac{p_0}{p_k} \right)^{R/c_p} \exp \left( \frac{L\bar{q}_k}{c_p \bar{T}_k} \right)$  at a given "departing" model level  $k_{\text{dep}}$ ; for parcels ascending in the lowest 30 hpa, mixed layer values are used. The CAPE value retained is the maximum value from the different ascents.

The Convective Inhibition (CIN) is estimated in analogy to CAPE by retaining the negative part of the integral

$$\text{CIN} = - \int_{z_{\text{dep}}}^{z_{\text{LFC}}} g \left( \frac{T_{\text{up}} - \bar{T}}{\bar{T}} \right) dz \approx - \int_{z_{\text{dep}}}^{z_{\text{LFC}}} g \left( \frac{\theta_{\text{e,up}} - \bar{\theta}_{\text{esat}}}{\bar{\theta}_{\text{esat}}} \right) dz; \quad \theta_{\text{e,up}} - \bar{\theta}_{\text{esat}} < 0 \quad (2.65)$$

where LFC is the Level of Free Convection, approximated as the level where CAPE exceeds a small threshold. CIN is therefore positive definite. The CIN value retained is the minimum value from the different ascents with  $\text{CIN} > 0$ .

## 12. Structure of code

The parameterization of cumulus convection is performed in subroutines shown in Fig. 2.1.

**CUCALLN:** Provides interface of routines for cumulus parametrization. It takes the input values through arguments from CALLPAR and returns updated tendencies of  $T, q, l, u, v$  and chemical Tracers, as well as convective precipitation rates.

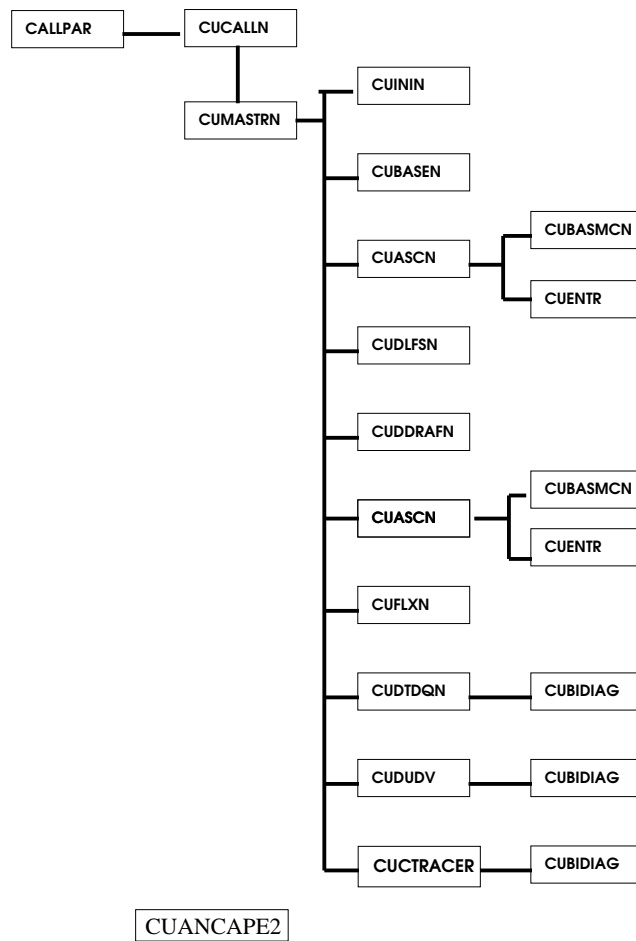


Figure 2.1: Structure of convection scheme.

**CUMASTRN**: Master routine for convection scheme. Also performs the convective closure and with Cy32r3 computes the momentum in the convective draughts.

**CUININ**: Initializes variables for convection scheme (including vertical interpolation to the half model levels).

**CUBASEN**: First Guess updraught. Calculates condensation level, and sets updraught base variables and first guess cloud type.

**CUASCN**: Calculates ascent in updraughts. Before Cy32r3 CUASCN has been called twice as part of an iterative procedure. With ccyle 32r3 CUASCN is only called once and the mass flux scaling is done in routine CUMASTRN. Routines CUENTR and CUBASMEN are called from CUASCN.

**CUENTR**: Calculates turbulent entrainment and detrainment rates.

**CUBASMEN**: Calculates cloud base properties of mid-level convection.

**CUDLFSN**: Calculates the level of free sinking for downdraughts.

**CUDDRAFEN**: Calculates the downdraught descent.

**CUFLXN**: Calculates final convective fluxes and surface precipitation rates taking into account of melting/freezing and the evaporation of falling precipitation.

**CUDTDQN**: Calculates the tendencies of  $T$  and  $q$  from convection.

**CUUDVDV**: Calculates the tendencies of  $u$  and  $v$  from convection.

**CUADJTQ**: Calculates super/sub saturation and adjusts  $T$  and  $q$  accordingly.

**CUCTRACER**: Calculates convective tendencies for chemical Tracers.

**CUBIDIAG**: Solver for bi-diagonal linear equation system.

**CUANCAPE2**: Computes CAPE diagnostics.

## EXTERNALS

Subroutine **SATUR** for calculating saturation mixing ratio.

## PARAMETERS

Defined in subroutine **SUCUM** called from INIPHY.

## Appendix A. List of symbols

CAPE	Convective available potential energy
CIN	Convective inhibition
$C^i$	Convective chemical Tracer no $i$
$C_{\text{down}}^i$	Convective Tracer concentration in updraught
$C_{\text{down}}^i$	Convective Tracer concentration in downdraught
$C_d$	Drag coefficient
$C_{\text{conv}}$	Fraction of grid square occupied by convection
$c_p$	Specific at constant pressure for dry air
$c_{\text{up}}$	Condensation/sublimation in the updraughts
$c_0$	Autoconversion coefficient
$D_{\text{up}}$	Rate of mass detrainment in the updraughts
$D_{\text{down}}$	Rate of mass detrainment in the downdraughts
$D_{\text{st}}$	Total kinetic energy dissipation in mmodel column
$E_{\text{up}}$	Rate of mass entrainment in the updraughts
$E_{\text{down}}$	Rate of mass entrainment in the downdraughts
$e^{\text{rain}}$	Evaporation of rain
$e_{\text{down}}$	Evaporation of precipitation (rain and snow) in the downdraughts
$e_{\text{down}}^{\text{rain}}$	Evaporation of rain in the downdraughts
$e_{\text{down}}^{\text{snow}}$	Evaporation of snow in the downdraughts
$\tilde{e}_{\text{subcld}}$	Evaporation of precipitation (rain and snow) in the unsaturated sub-cloud layer
$f_{\text{scale}}$	vertical scaling function for the entrainment
$\tilde{e}_{\text{subcld}}^{\text{rain}}$	Evaporation of rain in the unsaturated sub-cloud layer
$\tilde{e}_{\text{subcld}}^{\text{snow}}$	Evaporation of snow in the unsaturated sub-cloud layer
$F_{\text{rez}}$	Freezing rate of condensate in the updraughts
$g$	gravity constant
$G^{\text{precip}}$	Conversion rate from cloud (water+ice) into precipitation (rain+snow)
$G^{\text{rain}}$	Conversion rate from cloud water into rain
$G^{\text{snow}}$	Conversion rate from cloud ice into snow
$\bar{h}$	Moist static energy ( $= c_p \bar{T} + L\bar{q} + gz$ ) in the environment
$\bar{h}_{\text{sat}}$	Saturated moist static energy in the environment
$h_{\text{up}}$	Moist static energy in the updraughts
$h_{\text{down}}$	Moist static energy in the downdraughts
$J_s$	Surface turbulent sensible heat flux
$J_q$	Surface turbulent latent heat flux
$k$	model level
$K_{\text{up}}$	Kinetic energy in the updraughts
$L$	Effective latent heat for an ice/water mix
$L_{\text{fus}}$	Latent heat of fusion
$L_{\text{subl}}$	Latent heat of sublimation
$L_{\text{vap}}$	Latent heat of vaporization
CFL	Courant–Friedrich–Levy criterium
LCL	Lifting Condensation Level
LFC	Level of Free Convection
$l_{\text{up}}$	Cloud water/ice content in the updraughts
$l_{\text{crit}}$	Cloud water/ice content above which autoconversion occurs
$M_{\text{elt}}$	Melting rate of snow

$M_{\text{cld}}$	Net mass flux in the convective clouds (updraughts + downdraughts)
$M_{\text{up}}$	Net mass flux in the downdraughts
$M_{\text{down}}$	Net mass flux in the downdraughts
$n$	index for time discretization
$n_T$	horizontal truncation (global wavenumber)
$n_{\text{lev}}$	number of vertical model levels ( $n_{\text{lev}}$ denotes the first layer above surface)
$P^{\text{rain}}$	Net flux of precipitation in the form of rain
$P^{\text{snow}}$	Net flux of precipitation in the form of snow
$p$	Pressure
$p_0$	Reference pressure=1000 hPa
$\bar{q}$	Specific humidity of the environment
$q_{\text{up}}$	Specific humidity in the updraughts
$q_{\text{down}}$	Specific humidity in the downdraughts
$R$	Rain intensity
$RH$	Relative humidity
$r_{\text{up}}$	Precipitation (rain+snow) in the updraughts
$r_{\text{down}}$	Precipitation (rain+snow) in the downdraughts
$S_{\text{fallout}}$	Fall-out of rain/snow
$\bar{s}$	Dry static energy in the environment
$s_{\text{up}}$	Dry static energy in the updraughts
$s_{\text{down}}$	Dry static energy in the downdraughts
$\bar{T}_v$	Virtual temperature in the environment
$T_{v,\text{up}}$	Virtual temperature in the updraughts
$\bar{u}$	$u$ component of wind in the environment
$u_{\text{up}}$	$u$ component of wind in the updraughts
$u_{\text{down}}$	$u$ component of wind in the downdraughts
$u_{\text{pert}}$	additional updraught perturbation velocity
$\bar{V}$	Mean terminal velocity of precipitation (rain+snow)
$V_{\text{rain}}$	Mean terminal velocity of rain drops
$\bar{v}$	$v$ component of wind in the environment
$v_{\text{up}}$	$v$ component of wind in the updraughts
$v_{\text{down}}$	$v$ component of wind in the downdraughts
$\bar{w}$	Vertical velocity in the environment
$w_{\text{up}}$	Vertical velocity in the updraughts
$w_*$	Convective velocity scale
$\alpha_1, \alpha_2, \alpha_3$	Microphysical constants
$\alpha_n$	Horizontal resolution dependency of the deep convective adjustment time
$\alpha^{(s)}, \alpha^{(q)}$	Interpolation coefficients for half-level values
$\delta$	Detrainment per unit length
$\varepsilon$	Entrainment per unit length
$\eta$	Updraught mass flux fraction to initialise downdraught
$\kappa$	von Karman constant
$\rho$	Density of air
$\rho_{\text{rain}}$	Density of rain
$\tau$	Adjustment time scale
$\tau_m$	Melting time scale
$\omega$	Omega (large-scale) vertical velocity
$\Delta p$	Pressure difference between two model half-levels
$\Delta t$	Model time step

# Bibliography

- Arakawa, A. and W. H. Schubert, 1974: Interaction of a cumulus cloud ensemble with the large-scale environment. Part I. *J. Atmos. Sci.*, **31**, 674–701.
- Bechtold, P., J.-P. Chaboureau, A. Beljaars, A. K. Betts, M. Köhler, M. Miller, and J.-L. Redelsperger, 2004: The simulation of the diurnal cycle of convective precipitation over land in a global model. *Q. J. R. Meteorol. Soc.*, **130**, 3119–3137.
- Bechtold, P., M. Köhler, T. Jung, M. Leutbecher, M. Rodwell, F. Vitart, and G. Balsamo, 2008: Advances in predicting atmospheric variability with the ecmwf model, 2008: From synoptic to decadal time-scales. *Q. J. R. Meteorol. Soc.*, **130**, 3119–3137.
- Bennets, D. A. and B. J. Hoskins, 1979: Conditional symmetric instability—a possible explanation for frontal rainbands. *Q. J. R. Meteorol. Soc.*, **105**, 945–962.
- Bennets, D. A. and J. C. Sharp, 1982: The relevance of conditional symmetric instability to the prediction of meso-scale frontal rainbands. *Q. J. R. Meteorol. Soc.*, **108**, 595–602.
- Browning, K. A., M. E. Hardman, T. W. Harrold, and C. W. Pardoe, 1973: The structure of rainbands within a mid-latitude depression. *Q. J. R. Meteorol. Soc.*, **99**, 215–231.
- Cheng, L., T.-C. Yip, and H.-R. Cho, 1980: Determination of mean cumulus cloud vorticity from GATE A/B-scale potential vorticity budget. *J. Atmos. Sci.*, **37**, 797–811.
- Doms, G. and U. Schättler, 2004: A description of the nonhydrostatic regional model LM. Part II: Physical parameterization. Technical report, Deutscher Wetterdienst, Offenbach, (available from <http://www.cosmo-model.org/public/documentation.htm>).
- Emanuel, K. A., 1982: Inertial instability and mesoscale convective systems. Part II: Symmetric CISK in a baroclinic flow. *J. Atmos. Sci.*, **39**, 1080–1097.
- Field, P., R. Hogan, P. Brown, A. Illingworth, T. Choullartona, and R. Cotton, 2005: Parametrization of ice-particle size distributions for mid-latitude stratiform cloud. *Quart. J. Roy. Met. Soc.*, **131**, 1997–2017.
- Foster, D. S., 1958: Thunderstorm gusts compared with computed downdraught speeds. *Mon. Wea. Rev.*, **86**, 91–94.
- Fritsch, J. M. and C. G. Chappell, 1980: Numerical prediction of convectively driven mesoscale pressure systems. Part I: Convective parametrization. *J. Atmos. Sci.*, **37**, 1722–1733.
- Gregory, D.: 1997, Parametrization of convective momentum transports in the ECMWF model: evaluation using cloud resolving models and impact upon model climate. *Proc. ECMWF Workshop on New Insights and Approaches to Convective Parametrization*, 208–227, Reading, 4–7 November 1996.

- Gregory, D., R. Kershaw, and P. M. Inness, 1997: Parametrization of momentum transports by convection. II: Tests in single-column and general circulation models. *Q. J. R. Meteorol. Soc.*, **123**, 1153–1183.
- Herzogh, P. H. and P. V. Hobbs, 1980: The mesoscale and microscale structure and organization of clouds and precipitation in mid-latitude cyclones. Part II: Warm frontal clouds. *J. Atmos. Sci.*, **37**, 597–611.
- Hobbs, P. V. and A. L. Rangno, 1985: Ice particle concentrations in clouds. *J. Atmos. Sci.*, **42**, 2523–2548.
- Houze, R. A., J. D. Locatelli, and P. V. Hobbs, 1976: Dynamics and cloud microphysics of the rainbands in an occluded frontal system. *J. Atmos. Sci.*, **35**, 1921–1936.
- Jakob, C. and A. P. Siebesma, 2003: A new subcloud model for mass flux convection schemes. influence on triggering, updraught properties and model climate. *Mon. Wea. Rev.*, **131**, 2765–2778.
- Johnson, R. H., 1976: The role of convective-scale precipitation downdrafts in cumulus and synoptic scale interactions. *J. Atmos. Sci.*, **33**, 1890–1910.
- 1980: Diagnosis of convective and mesoscale motions during Phase III of GATE. *J. Atmos. Sci.*, **37**, 733–753.
- Kessler, E., 1969: *On the distribution and continuity of water substance in atmospheric circulation*, volume 10 of *Meteorological Monographs*. Am. Meteorol. Soc., Boston, MA.
- Kuo, H. L. and W. H. Raymond, 1980: A quasi-one-dimensional cumulus cloud model and parametrization of cumulus heating and mixing effects. *Mon. Wea. Rev.*, **108**, 991–1009.
- Le Mone, M. A. and W. T. Pennell, 1976: The relationship of trade wind cumulus distribution to subcloud layer fluxes and structure. *Mon. Wea. Rev.*, **104**, 524–539.
- Lin, Y.-L., R. D. Farley, and H. Orville, 1983: Bulk parameterization of the snow field in a cloud model. *J. Clim. Appl. Meteorol.*, **22**, 1065–1092.
- Lindzen, R. S., 1981: Some remarks on cumulus parametrization. *Rep. on NASA-GISS Workshop: Clouds in Climate: Modelling and Satellite Observational Studies*, 42–51.
- Liu, J. Y. and H. D. Orville, 1969: Numerical modeling of precipitation and cloud shadow effects on mountain-induced cumuli. *J. Atmos. Sci.*, **26**, 1283–1298.
- Mason, B. J., 1971: *The Physics of Clouds*. Clarendon Press.
- Meyers, M. P., P. J. DeMott, and W. R. Cotton, 1992: New primary ice-nucleation parameterizations in an explicit cloud model. *J. Appl. Met.*, **31**, 708–721.
- Nordeng, T.-E., 1994: Extended versions of the convection parametrization scheme at ECMWF and their impact upon the mean climate and transient activity of the model in the tropics. *ECMWF Tech. Memo. No. 206*.
- Seifert, A. and K. D. Beheng, 2001: A double-moment parameterization for simulating autoconversion, accretion and selfcollection. *Atmos. Res.*, **59-60**, 265–281.
- Simpson, J., 1971: On cumulus entrainment and one-dimensional models. *J. Atmos. Sci.*, **28**, 449–455.

Simpson, J. and V. Wiggert, 1969: Models of precipitating cumulus towers. *Mon. Wea. Rev.*, **97**, 471–489.

Steinheimer, M., M. Hantel, and P. Bechtold, 2007: Convection in Lorenz's global energy cycle with the ECMWF model. *Tellus*, **60A**, 1001–1022.

Sundqvist, H., 1978: A parameterization scheme for non-convective condensation including prediction of cloud water content. *Q. J. R. Meteorol. Soc.*, **104**, 677–690.

Wexler, R. and D. Atlas, 1959: Precipitation generating cells. *J. Meteorol.*, **16**, 327–332.